Appl. Phys. A 69 [Suppl.], S633–S636 (1999) / Digital Object Identifier (DOI) 10.1007/s003399900366

Applied Physics A
Materials
Science & Processing

High rate deep channel ablative formation by picosecond–nanosecond combined laser pulses

S.M. Klimentov[1], S.V. Garnov[1], T.V. Kononenko[1], V.I. Konov[1], P.A. Pivovarov[1], F. Dausinger[2]

[1] General Physics Institute of the Russian Academy of Sciences, 117942 Moscow, Vavilov str. 38
(Fax: +7-095/234-9022, E-mail: kliment@kapella.gpi.ru)
[2] Institut für Strahlwerkzeuge, Pfaffenwaldring 43, D-70569 Stuttgart, Germany
(Fax: +49-0711/685-6842)

Received: 5 October 1999/Accepted: 5 October 1999/Published online: 28 December 1999

Abstract. Temporally profiled pulsed radiation of the Nd:YAG laser was applied to drilling and micromachining of ceramics, steel, and CVD diamond, demonstrating one or two orders of magnitude enhancement of ablation rates compared to conventional pico- and nanosecond-pulsed ablation at the same energy density. The developed laser system delivered combined pulses consisting of a picosecond pulse train followed by a nanosecond pulse train. The combination of picosecond and nanosecond components within one laser shot turned out to be especially beneficial for high-aspect-ratio channel formation. Polarization dependence of the ablated deep crater morphology was observed in AlN samples. Waveguide radiation propagation in self-made deep channels as well as the influence of high-temperature laser-produced plasma on this phenomena are discussed.

PACS: 42.62.Cf; 42.60.By

Shielding of an irradiated area by laser-produced plasma is one of the key problems for high-rate precision ablation by intense, short (picosecond and nanosecond) pulses. In the case of deep channel formation, the problem looks even more complicated: the plasma at the bottom is denser due to expansion limitations imposed by the side walls [1]. The use of femtosecond pulses could be one of the solutions to minimize plasma shielding [2, 3]. Another possibility, considered in this paper, is application of pulse trains including picosecond and nanosecond components. Indeed, plasma parameters can be dramatically changed by a proper choice the intensity and time interval between pulses and, correspondingly, the influence of shielding on ablation can be modified or even suppressed. The combination of pulses of different duration and intensity within one laser shot allows more than the reduction of plasma shielding. An important resort for the improvement of ablation efficiency in the channels is "casting roles" between the particular components of the pulse succession. The initial pulse (or several pulses) is able to modify ablation conditions for the following portions of radiation (to lower ablation threshold, for instance), while the train of short laser pulses at the end of the succession can promote removal of the ablated material.

COLA'99 – 5th International Conference on Laser Ablation, July 19–23, 1999 in Göttingen, Germany

1 Experimental setup

For the ablation tests, we specially developed the Nd:YAG laser, operating in the combined pulse mode, so that within a single pumping pulse the laser output consisted of an initial train of picosecond pulses with an axial period of 3.5 ns which, after a time delay of $\sim 10\,\mu$s, was followed by a sequence of 10–20 Q-switched 200 ns pulses with a period of 5–7 μs. Using a wide-band oscilloscope and fast photodiode, we estimated the energy of the picosecond component to be the largest in the combined pulse train and thus the nanosecond pulses were much less intensive. Parameters of the temporally profiled pulse are shown schematically in Fig. 1. After amplification and spatial filtering, the total shot energy amounted to 20 mJ with the pulse-to-pulse energy spread below 5%. The entire device allowed operation at the maximum repetition rate of 10 Hz.

A single transverse mode beam was focused at the sample surface with 65–115-mm focal length lenses which corresponded to the irradiated spot diameters $d_s = 25$–$45\,\mu$m. The

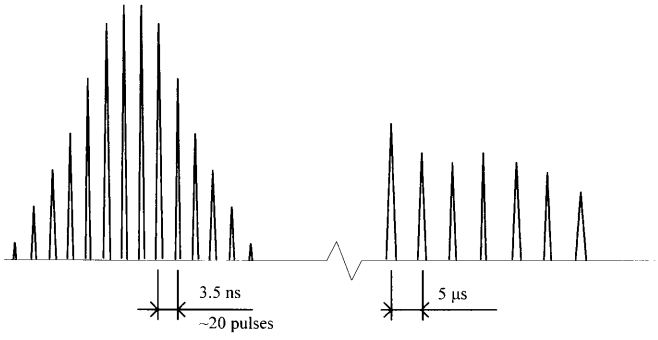

Fig. 1. Schematic of the combined picosecond–nanosecond pulse structure

sample plates (up to 1.2 mm thick) were made of ceramics (AlN in most of the experiments), stainless steel, and CVD diamond. The samples were positioned at the input window of a photometric sphere and exposed to ablative pulses until the through hole was created. In the course of drilling, the incident E_0 and transmitted E_t energy signals were recorded by AD converters to obtain the ratio. The idea of integrating sphere registration was to define correctly the number of pulses N_1, needed to produce a through hole in the opaque sample, and the number of pulses N_2, corresponding to formation of the largest exit diameter (d_t); formation, and to measure the maximum transmission of laser radiation through the ablated channel by the E_t/E_0 ratio.

2 Results and discussion

Radiation transmission dynamics for the 1.2 mm AlN sample is given in Fig. 2 as an example. As can be seen, at the energy density of 1200 J/cm^2 the output hole appears after about 200 pulses (N_1) which corresponds to a very high drilling rate of ~ 6 μm/pulse. The following process of the through channel formation manifests itself by transmission growth with oscillations, indicating successive cleaning and clogging of the output hole, and finally stops at $N_2 \approx 500$. No plasma is observed at this point and the final transmission E_t/E_0 reaches the 20% level which means that most of the laser energy is absorbed inside the channel.

The losses measured are rather high which is consistent with the geometry of the channels drilled in AlN at the typical focusing parameters ($d_s = 25$ μm, $1/e$ – intensity level). The input hole diameter d_0 was close to d_s, the aspect ratio (h/d_0) amounted to 40, and in all cases the output hole size d_t appeared to be less than the input ($d_t < d_0$). Considering altogether the transmission data, the characteristic input and output hole diameters, the focused beam geometry, and the significant thickness of the ablated plates, we come to the conclusion that for AlN ceramics a kind of waveguide beam propagation takes place in the self-created channel with high losses which, specifically, results in its conical shape.

The pronounced polarization dependence, observed in the special tests implying linear and circular polarized beams, confirms this idea. As follows from the microscope observation (Fig. 3), this dependence manifests itself in the output hole shape. While the entrance hole is round, disregarding the incident beam polarization (Fig. 3a), the opening at the rear surface is strongly polarization dependent. It is circular with $d_t < d_0$ for the circular polarized beam (Fig. 3c) or shaped as a narrow slit in the case of linear polarization. Orientation of the slit here is strictly perpendicular to the plane of polarization (Fig. 3b). To obtain the result shown in Fig. 3b we rotated the polarization plane within an angle of 90°. In the same tests steel samples demonstrated no apparent polarization dependence, neither in the ablation rate, nor in the channel morphology, which is consistent with less pronounced angular dependence of the surface optical properties in metals [4].

The results described differ drastically from our ablation data obtained for conventional intense pico- and nanosecond single pulses. It can be illustrated by transmission dependence, measured in a 170 μm thick semitransparent sample of AlN ceramics, ablated by 2 ns pulses at the energy density of 500 J/cm^2 (Fig. 4). The transmission registration schematic was the same as mentioned above ($T = E_t/E_0$). Shown on the graph are transmission values of two sorts. So-called "hot" transmission T_H was measured in the course of ablative channel formation, i.e., in the presence of hot laser plasma at the surface, the "cold" transmission T_C was measured between the "hot" series with probe low intensity pulses below the ablation and plasma formation threshold. Due to significant plasma shielding, the "hot" readings are much lower than the "cold" ($T_H \ll T_C$).

Collation of the graph in Fig. 2 and the $T_C(N)$ curve in Fig. 4 reveals similar behavior except for two very import-

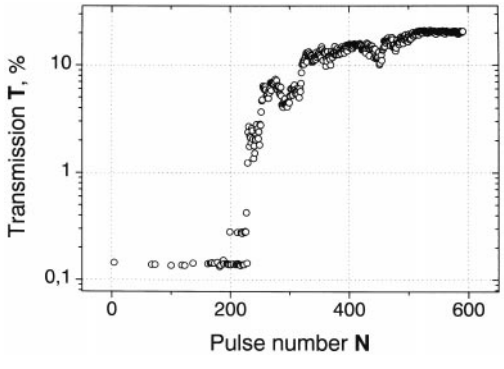

Fig. 2. Transmission plot for the channel, ablated in AlN opaque sample (thickness, 1.2 mm; input/output diameters, 30/10 μm) at the energy density of 1200 J/cm^2 (circular polarization of incident radiation). Obtained from the graph are: the average ablation rate of 5.5 μm/pulse; output hole completing pulses $N_2 \approx 500$; optical losses in the channel of 80%

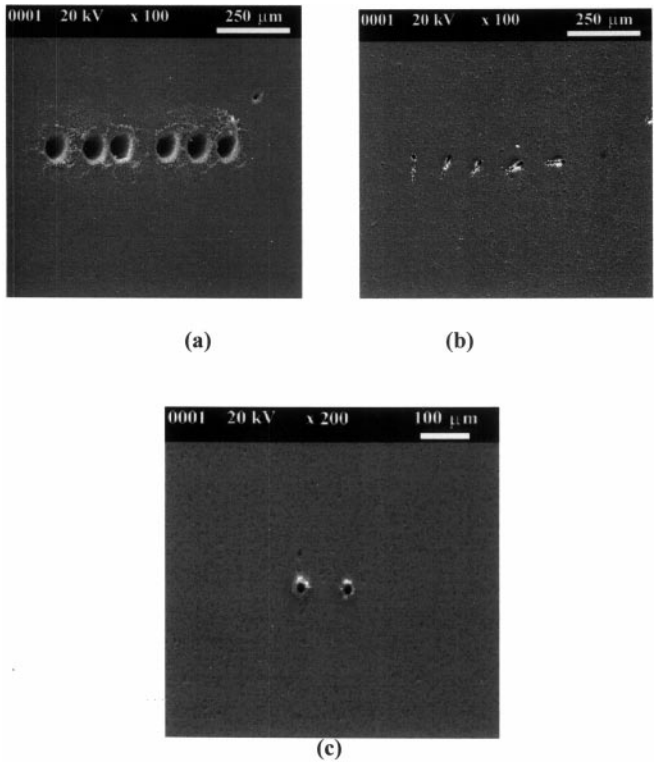

Fig. 3a–c. Polarization dependence of the output hole shape observed in AlN ceramics. Input (**a**) and rear surface holes (**b**) exposed to the incident radiation of different orientations of the polarization plane. (**c**) The holes produced by circular polarized beam

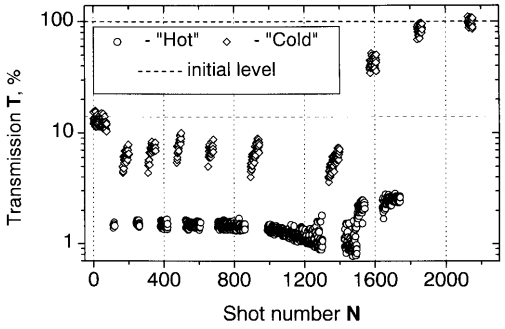

Fig. 4. Transmission dependence in semitransparent AlN ceramics ablated by 2 ns laser pulses

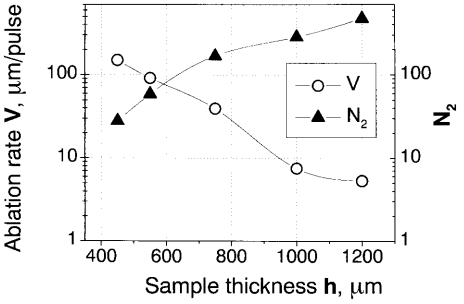

Fig. 5. Average ablation rates (*open circles*) and pulse numbers, corresponding to completion of drilling in AlN ceramics (*solid triangles*)

ant points: the complete perforation of the sample by conventional nanosecond single pulses at $N \approx 2000$ results in $\sim 100\%$ channel transmission for the ceramics tested and $d_t \approx d_0 \gg d_s$, while for the combined pulse drilling the final transmission level does not exceed 20% even for the maximum achievable exit diameters $d_t < d_0$ (for the transmission curve in Fig. 2, $T_H = T_C$ when $N > N_2$). It is evident from these facts that in the case of high intensity nanosecond single pulses, wave guide propagation may not occur, and the surface plasma can play a most important role in the beam intensity attenuation. Such laser plasma expands and interacts with the channel walls which can drastically increase the ablated channel diameter [1] making it much larger than the focused spot, at least for ceramics. Concerning this channel enlargement, one should keep in mind that in the described nanosecond pulse experiment the resulting crater size ($d_0 = 200$ μm for $d_s = 50$ μm) exceeds the beam diameter, estimated by calculating the Gaussian beam size, within which the intensity is above the ablation threshold.

It is also worth mentioning that the "hot" and "cold" curves in Fig. 4 are practically constant until the exit opening formation at $N > 1400$, which indicates that conditions for surface plasma generation do not change much with the channel depth. Simple estimation also shows that the intensity in an individual nanosecond spike of the combined pulse train (for the same total energy fluence) is at least two orders of magnitude lower than for a typical nanosecond single pulse ($\tau \sim 20 \div 40$ ns) which should result in significantly more transparent (less dense) surface plasma, much higher ablation rates, the channel diameters much closer to d_s, and domination of waveguide propagation losses in the energy balance.

Visual observations of the spot, irradiated by the combined pulses, have shown that at the flux level below 1200 J/cm^2 plasma brightness is much lower than for pico- and nanosecond single pulses. This can be considered as additional evidence for the pronounced difference between the single and combined short pulse regimes of deep hole penetration discussed above: absence in the later case of the strong shielding plasma leads to much higher ablation rates and channel diameters significantly closer to d_s.

Application of the transmission measurement procedure to the combined pulse ablation in AlN samples of different thickness h_0 resulted in the graph in Fig. 5. The calculated average ablation rates $V = h_0/N_1$ are plotted here along with the pulse numbers N_2, corresponding to drilling completion. Compared to the conventional pulsed ablation data [5, 6], the combined mode demonstrated faster (by two orders of magnitude) drilling for the same thickness, focusing spot, and energy density. In the same way, advantages of the combined pulse mode were demonstrated for the other materials investigated. Attracts attention also the difference in $V(N)$ behavior for the combined and single pulse drilling. Typically, in the later case, there are two characteristic regions with approximately constant ablation rates: the fast one at the beginning of crater formation switching to the slow one at a definite channel depth. The $V(N)$ dependence shown in Fig. 6 can be attributed to shifting of the plasma-shielding regime. The ablation rate for the combined pulse mode slows gradually with the channel length demonstrating no clear steps, which may indicate the domination of Fresnel losses in a waveguide-like deep structure. The drilling of steel also revealed fast rates comparable to those in ceramics (see Fig. 7). In the same way as for ceramics, we could not avoid the conical shape of the

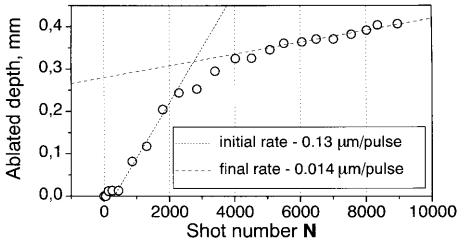

Fig. 6. Ablated depth dependence obtained in 0.6 mm thick Al_2O_3 ceramics, exposed to 2 ns pulses at the laser flux of 600 J/cm^2 ($d_s = 40$ μm)

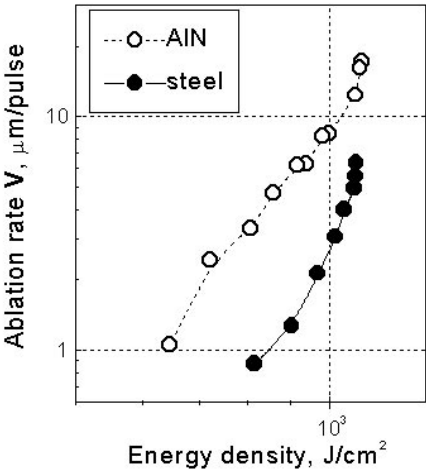

Fig. 7. Ablation rates measured in 1-mm sample plates versus incident energy density: steel (*closed circles*) and ceramics of AlN (*open circles*)

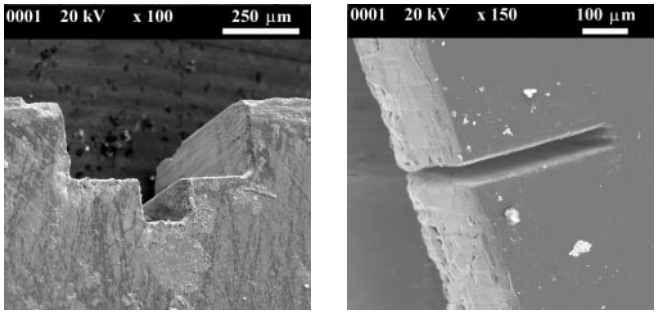

Fig. 8. a Through cuts in 0.75 mm AlN ceramics and **b** 0.5 mm thick CVD diamond film

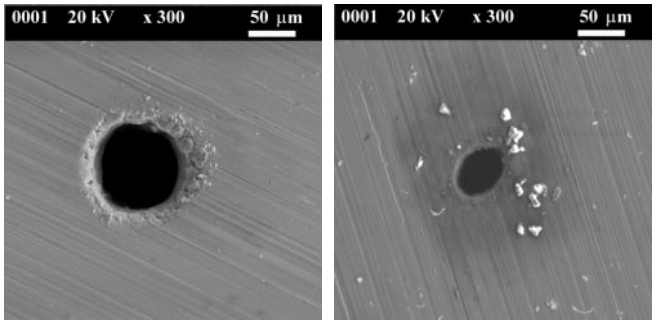

Fig. 9. a Front and **b** rear surface of 1 mm thick steel plate after trepanning-like drilling at the energy density of 2500 J/cm^2 (3500 pulses)

created channel ($d_{\text{inp}} = 30\,\mu\text{m}$, $d_{\text{out}} = 20\,\mu\text{m}$), which may additionally stands for the suggestion on dominating radiation transport losses and deficiency of the incident energy accumulation in plasma.

The observed advantages and peculiarities of the combined picosecond–nanosecond laser pulse trains provide good prospects for high-rate and high-precision materials microstructuring which is illustrated by the through cuts and deep structures in the AlN and CVD diamond samples shown in Fig. 8. Promising results have been also achieved in formation of high-aspect-ratio through holes by a trepanning-like method, which implied gyration of the sample plate in the course of pulsed drilling, so that the diameter of gyration approximately matched or slightly exceeded the focused spot diameter. Pronounced spatial profile overlapping took place here. Figure 9 shows results of the trepanning procedure in 1 mm thick steel.

3 Conclusions

It is shown that the combination of picosecond and nanosecond pulse trains within one shot of Nd:YAG laser provides 1–2 orders of magnitude higher ablation rates in shallow and deep channels compared to conventional pico- and nanosecond single pulses of the same fluence (below the level of 1200 J/cm^2). This opens wide possibilities for application of such lasers in materials micromachining. The dynamics of deep hole penetration and optical transmission of the laser-produced channel were investigated. It is evident from the obtained results that, depending on the pulse temporal shape, either waveguide propagation, corresponding to the minimum plasma influence and domination of the energy transport losses in the channel, or plasma assisted mode, implying significant plasma shielding and side-wall ablation, could be realized. More refined experiments, allowing direct comparison of the plasma-screening effect for the combined and conventional laser pulses, are in progress.

References

1. S.V. Garnov, S.M. Klimentov, V.I. Konov, T.V. Kononenko, F. Dausinger: Russ. J. Quantum Electron. **QE-28**, 42 (1998)
2. A. Luft, U. Franz, A. Emsermann, J. Kaspar: Appl. Phys. A **63**, 93 (1996)
3. T.V. Kononenko, V.I. Konov, S.V. Garnov, R. Danielius, A. Piskarskas, G. Tamoshauskas, F. Dausinger: Kvantovaya Electronika (Russian) **28**, 167 (1999)
4. R.M.A. Azzam, N.M. Bashara: *Ellipsometry and Polarized Light* (North Holland, Amsterdam, New York, Oxford 1977)
5. T.V. Kononenko, S.V. Garnov, S.M. Pimenov, V.I. Konov, F. Dausinger: Proc. SPIE **3343**, 458 (1998)
6. T.V. Kononenko, S.V. Garnov, S.M. Klimentov, V.I. Konov, E.N. Loubnin, F. Dausinger, A. Raiber, C. Taut: Appl. Surf. Sci. **109–110**, 48 (1997)